PROCEEDINGS OF SCIENCE

A study of the radio frequency spectrum emitted by high-energy air showers with LOFAR

L. Rossetto[1]*, S. Buitink[2], A. Corstanje[1], J.E. Enriquez[1], H. Falcke[1,3,4], J.R. Hörandel[1,3], A. Nelles[1,5], J.P. Rachen[1], P. Schellart[1], O. Scholten[6,7], S. ter Veen[1,4], S. Thoudam[1], T.N.G. Trinh[6]

[1] *Department of Astrophysics / IMAPP, Radboud University Nijmegen, P.O. Box 9010, 6500 GL, Nijmegen, The Netherlands*
[2] *Astrophysical Institute, Vrije Universiteit Brussel, Pleinlaan 2, 1050 Brussels, Belgium*
[3] *NIKHEF, Science Park Amsterdam, 1098 XG Amsterdam, The Netherlands*
[4] *Netherlands Institute of Radio Astronomy (ASTRON), Postbus 2, 7990 AA Dwingeloo, The Netherlands*
[5] *Now at: Department of Physics and Astronomy, University of California Irvine, Irvine, CA 92697-4575, USA*
[6] *KVI-CART, University Groningen, P.O. Box 72, 9700 AB Groningen, The Netherlands*
[7] *Interuniversity Institute for High-Energy, Vrije Universiteit Brussel, Pleinlaan 2, 1050 Brussels, Belgium*
E-mail: l.rossetto@astro.ru.nl

The LOw Frequency ARray (LOFAR) is a multipurpose radio antenna array aimed to detect radio signals in the frequency range $10 - 240$ MHz, covering a large surface in Northern Europe with a higher density in the Northern Netherlands. The detection of the radio signal emitted by extensive air showers allows to reconstruct the geometry of the observed cascade. Thus, several properties of primary particles (e.g. arrival direction, mass composition) can be inferred. We describe a study of several geometrical parameters of the radio signal emitted by extensive air showers propagating in the atmosphere, and their correlation with the observed radio frequency spectrum. In order to find the best parameters that describe the correlation between primary cosmic ray information and the emitted radio signal, a preliminary study on simulated events has been done. Monte Carlo simulations of radio signals have been produced by using the CoREAS code, a plug-in of the CORSIKA particle simulation code. The final aim of this study is to find a method to infer information of primary cosmic rays in an independent way from the well-established fluorescence and surface detector techniques, in view of affirming the radio detection technique as reliable method for the study of high energy cosmic rays.

The 34th International Cosmic Ray Conference,
30 July – 6 August, 2015
The Hague, The Netherlands

*Speaker.

© Copyright owned by the author(s) under the terms of the Creative Commons Attribution-NonCommercial-ShareAlike Licence.

PoS(ICRC2015)381

1. Introduction

Radio emission from extensive air showers was detected for the first time by Jelley et al. in 1965 [1]. Since 2005 radio experiments like CODALEMA [2] and LOPES [3] started detecting air showers up to an energy of 10^{18} eV, thus confirming the radio emission mechanisms of cosmic rays in the Earth atmosphere. In the last years, new measurements have been performed with the LOFAR experiment [4], and improvement in the understanding of radio emission processes of extensive air showers has been made.

First studies of radio frequency spectra below 100 MHz were conducted in late 1960s and early 1970s [5]. Analytical calculations [6, 7] and simulation studies [8] conducted at the beginning of years 2000 already showed a dependence of the radio frequency spectrum on cosmic ray air shower characteristics. Previous measurements of the frequency spectrum performed by LOPES did not show any significant dependence of the frequency spectrum with respect to the electric field strength, distance to the shower axis and arrival direction [9].

In view of extending these measurements to all data detected by LOFAR since 2011, a preliminary simulation study of the radio frequency spectrum has been conducted, and is presented here. The LOFAR array is briefly described in section 2. Radio emission processes of cosmic rays are introduced in section 3. Simulation analysis and corresponding results are presented in section 4. Conclusions and outlook are summarized in section 5.

2. LOFAR

The LOw Frequency ARray (LOFAR) is a radio antenna array which consists of 48 stations spread in Northern Europe with a more dense core in the Northern Netherlands. Each station consists of a set of Low Band Antennas (LBAs) and High Band Antennas (HBAs) which operate in the frequency range $10 - 90$ MHz and $110 - 240$ MHz, respectively. The 24 stations which form the LOFAR core are located in the Northern Netherlands, in the province of Drenthe, and cover a circle of 2 km radius approximately. All Dutch stations consist of 96 LBAs, subdivided into groups of 48 *inner* and 48 *outer* antennas, and 48 HBAs. The International stations consist instead of 96 LBAs and 96 HBAs. In the central area, a core of six stations, also called *Superterp*, are located in a circular area of roughly 320 m diameter, and form the most dense area of antennas. The layout of LOFAR central stations is shown in figure 1, together with a picture of one LBA. The LOFAR central array is also instrumented with 20 scintillator detectors, the LORA array [10]. Triggers for cosmic ray data acquisition are provided by LORA, which also permits to reconstruct the arrival direction and energy of primary particles. The LOFAR array allows to detect cosmic rays in the energy range $10^{16} - 10^{18}$ eV.

Measurements of cosmic rays are performed mostly by using signals from LBAs. The LBAs are designed to operate between 10 MHz, where the ionospheric cut-off of radio wavelengths takes place, and 90 MHz where the commercial FM radio band starts. Nevertheless, due to the presence of strong Radio Frequency Interference (RFI) at the lowest frequencies, and the proximity of the FM band at the highest ones, the LBA operational range is limited between $30 - 80$ MHz. Each LBA consists of two orthogonal dipole arms which are sensitive to two linear polarizations according to their orientation, i.e. NE $-$ SW for the X dipole, and NW $-$ SE for the Y one. The two

PoS(ICRC2015)381

dipole arms are 1.38 m long which corresponds to a resonance frequency of 52 MHz. However, the additional impedance of the amplifier shifts the resonance peak of the response curve to 58 MHz.

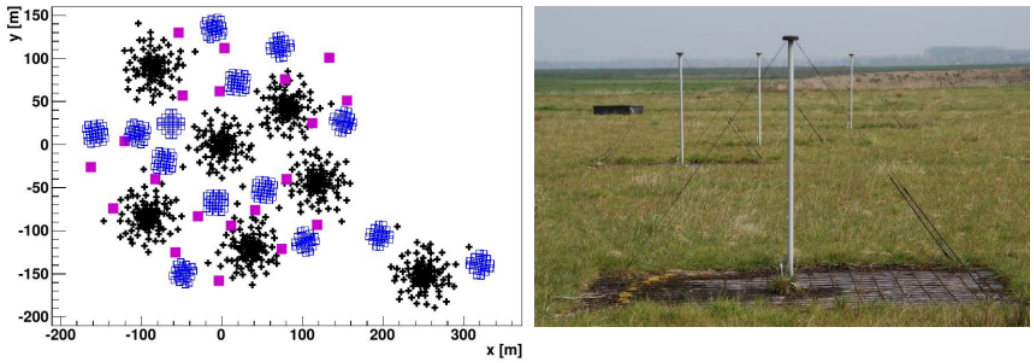

Figure 1: *Left*: layout of LOFAR central stations. The six stations on the left represent the *Superterp*. The location of LBA inner and outer antenna set is depicted as black crosses; the position of the HBAs is shown as well (open blue squares). The magenta squares indicate instead the LORA scintillator detectors. *Right*: picture of a LBA [11].

3. Radio emission process of extensive air showers

Secondary charged particles, produced in the atmosphere by the interaction of primary cosmic rays with the atmospheric nuclei, emit radio signals. Radio emission is generated by two mechanisms, the *geomagnetic* and the *charge excess process*. In the *geomagnetic process*, secondary electrons and positrons in the cascade are accelerated in opposite directions due to the Earth magnetic field. This effect creates a current which is linearly polarized in the direction perpendicular to the shower axis and to the geomagnetic field. In the *charge excess process* (also called *Askaryan effect* [12]), the radio emission is instead produced by a negative charge excess created by knocked-out electrons at the shower front. In this latter case, the negative charge excess is caused by electrons which are knocked-out by an energy transfer from shower particles to the air molecules. These electrons start moving with the cascade, thus leaving positive ions behind. Moreover, the secondary positrons annihilate with the electrons, thus creating a negative charge excess at the shower front. The radiation emitted due to the *charge excess process* is polarized in the radial direction with respect to the shower axis. Thus, the combination of these two mechanisms creates an asymmetric distribution of the total radio signal around the shower axis (see figure 2) [13, 14].

4. Simulation study of the frequency spectrum

The aim of this analysis is to study how the radio signal emitted by an extensive air shower is related to the arrival direction, energy and type of the primary particle.

The analysis has been conducted first on simulated showers. Simulations have been produced by using CORSIKA 7.400 [15] with the hadronic interaction models FLUKA 2011.2b [16] and QGSJETII.04 [17], and protons as primary particles. The additional radio emission simulation package CoREAS [18] has been used as a plug-in for CORSIKA. The antenna layout has been chosen in order to have a symmetric star-shape around the shower axis, in the plane perpendicular

PoS(ICRC2015)381

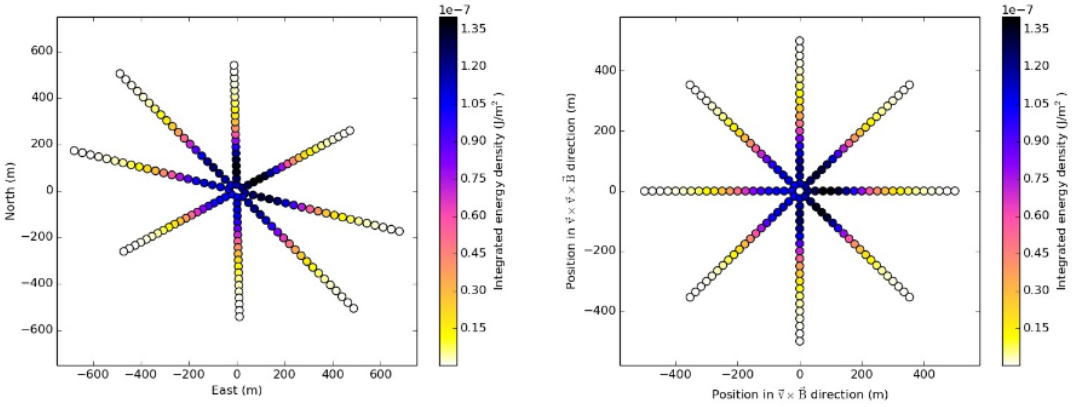

Figure 2: Integrated energy density for one simulated shower. The shower has an energy E = $2.04 \cdot 10^{18}$ eV, and an arrival direction with zenith angle $\theta = 46.73°$ and azimuth angle $\varphi = 239.4°$ (measured counter-clockwise starting from the North direction). *Left*: antenna layout projected at the ground level. *Right*: antenna layout as seen on the shower plane, where the centre corresponds to the position of the shower axis; the asymmetric distribution of the integrated radio signal around the shower axis is clearly visible.

to both the shower axis and the geomagnetic field (hereafter, *shower plane*). Simulations have been produced considering 160 antennas, distributed on 8 arms at an angle distance $\alpha = 45°$ between each other in the shower plane. Each antenna is 25 m distant from the previous one, thus covering an area of 500 m radius around the shower axis. Furthermore, the signal intensity in the time-domain is converted to the frequency-domain by applying a Fast Fourier Transform (FFT). The FFT distribution, as function of frequency, is then study for different cascade characteristics.

Figure 2 shows the antenna configuration used in this analysis, and the integrated pulse power (i.e. energy density) at each antenna for one single simulated event. The asymmetric antenna layout at the ground level (figure 2-*left*) becomes symmetric around the shower axis in the shower plane (figure 2-*right*). Furthermore, the asymmetric distribution of the integrated radio signal due to the interplay between the geomagnetic and charge excess process is clearly visible.

The asymmetric distribution of the integrated radio signal around the shower axis is also visible on the FFT distribution. Figure 3 shows the FFT distribution for the same simulated event shown in figure 2, and for seven antennas positioned along the $\vec{v} \times \vec{B}$ direction at $\alpha = 0°$, in the frequency range $30 - 80$ MHz. Starting from the antenna closest to the shower axis (i.e. at r = 25 m) and moving outwards, the FFT distribution becomes flatter until around 100 m from the shower axis, where radio emission reaches its maximum intensity. Continuing further outwards, the radio signal intensity decreases and, as a consequence, the FFT decreases as the frequency increases [19].

In order to describe the FFT distribution behaviour, the percentile statistical method has been used. The FFT distribution has been integrated in the frequency range $30 - 80$ MHz. In this frequency range, the percentile indicates the frequency value at which the integrated FFT distribution reaches a certain percent of the total integral. In the analysis described here, different values of percentile have been evaluated. Figure 4 shows the frequency distribution for all the 160 antennas in the shower plane considering the 30^{th} percentile (*left*), 50^{th} percentile (*centre*) and 70^{th} per-

PoS(ICRC2015)381

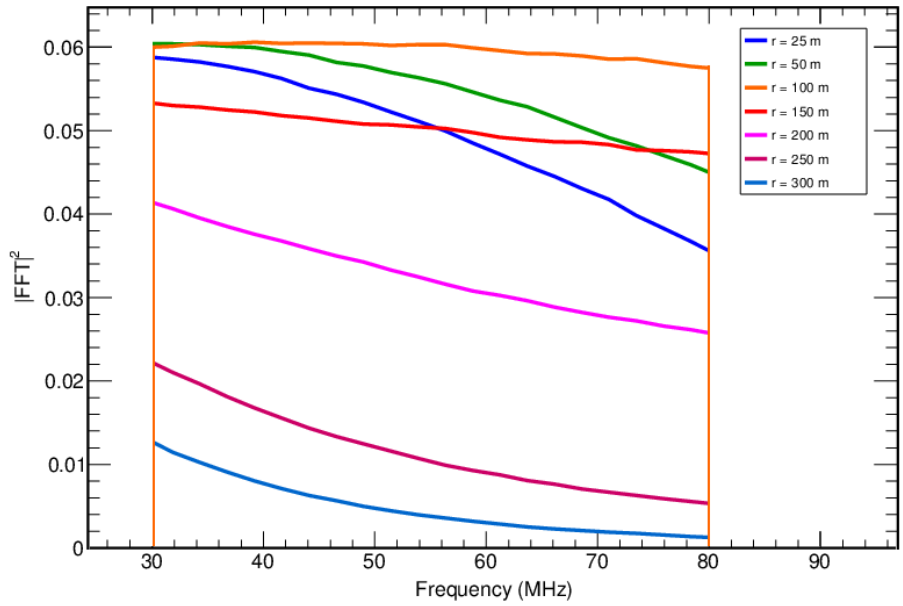

Figure 3: Distribution of the FFT as function of frequency for seven antennas positioned along the $\vec{v} \times \vec{B}$ direction at $\alpha = 0°$, and at different distances from the shower axis. The shower has an energy E = $2.04 \cdot 10^{18}$ eV, and an arrival direction with zenith angle $\theta = 46.73°$ and azimuth angle $\varphi = 239.4°$ (measured counter-clockwise starting from the North direction).

centile (*right*). Frequency values on the full shower plane have been evaluated through a polar coordinate interpolation, in order to better visualize any structure. Figure 4 clearly displays that the FFT distribution depends on the distance to the shower axis. Furthermore, it shows that the 50th percentile describes better the slope changing of the FFT distribution, in particular at a distance $\leq$ 50 m and above 200 m to the shower axis.

Considering the same starting conditions (i.e. energy and arrival direction) of the previously shown simulated event, the frequency spectrum was also studied by repeating the simulation for different values of X_{max} , i.e. the depth in the atmosphere where the cascade development reaches its maximum in terms of secondary particles produced. It has already been demonstrated, in previous simulation studies, that the size of the signal distribution around the shower axis in the shower plane decreases as X_{max} increases [20]. A similar result has been obtained in this analysis as well. Figure 5 shows the frequency distribution obtained considering the 50th percentile for three different values of X_{max} . It is clearly visible that, as X_{max} increases, the frequency distribution at the 50th percentile changes accordingly. This means that, as X_{max} increases, the FFT distribution starts decreasing closer to the shower axis.

This effect is also visible by considering the FFT distribution only for antennas at 200 m and 300 m from the shower axis, and for different simulated events. Figure 6 shows the frequency distribution of the 50th percentile as function of X_{max} for all the forty simulated events. For each event, the frequency of the 50th percentile has been evaluated as the average of the antennas at 200 m distance (*left*), and 300 m distance (*right*) from the shower axis. Figure 6 clearly shows that

PoS(ICRC2015)381

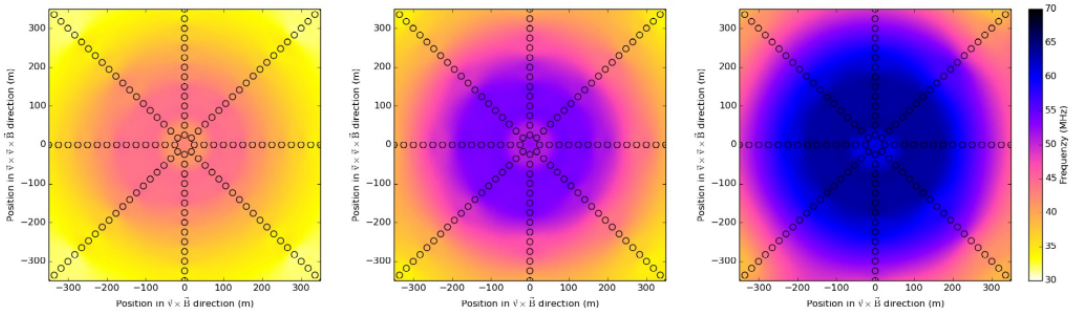

Figure 4: Frequency distribution for all the 160 antennas and for one simulated event. The event has an energy E = 2.04 · 10^{18} eV, and an arrival direction with zenith angle θ = 46.73° and azimuth angle φ = 239.4° (measured counter-clockwise starting from the North direction). The frequency distribution corresponds to the 30$^{\text{th}}$ percentile (*left*), 50$^{\text{th}}$ percentile (*centre*), and 70$^{\text{th}}$ percentile (*right*). Frequency values on the full shower plane have been evaluated through a polar coordinate interpolation.

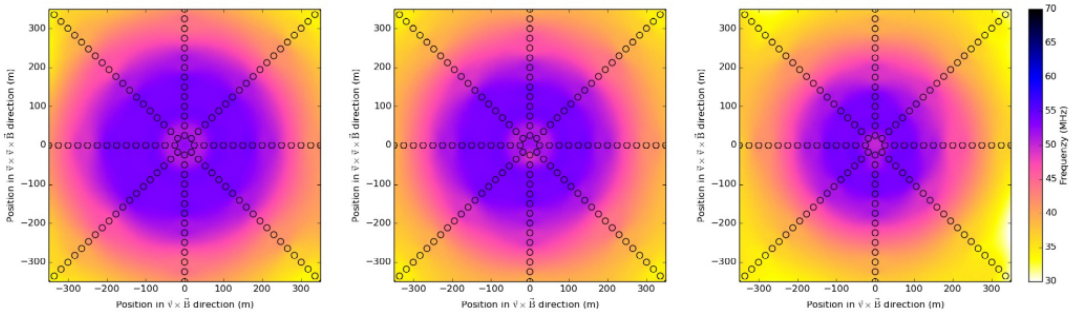

Figure 5: Frequency distribution of the 50$^{\text{th}}$ percentile for three simulated events and for all the 160 antennas. The starting conditions of the three events were: energy E = 2.04 · 10^{18} eV, zenith angle θ = 46.73° and azimuth angle φ = 239.4°. The plots referred to three different values of X_{max} : 660.24 g/cm^2 (*left*), 740.42 g/cm^2 (*centre*), 907.20 g/cm^2 (*right*).

the frequency of the 50$^{\text{th}}$ percentile decreases as X_{max} increases. The percentile statistical method can be then used to study the frequency spectrum behaviour. This method will be then applied in further simulation studies about the FFT distribution as function of primary particle characteristics.

5. Conclusions and outlook

The goal of the study here presented is to find a correlation between radio signals emitted by extensive air showers and arrival direction, energy and type of primary particles. A preliminary analysis have been conducted so far on simulated events, by studying the radio signal in the frequency-domain. The first part of the analysis consisted in choosing an appropriate parameter for describing the frequency spectrum at different distances to the shower axis. It has been demonstrated that the percentile statistical method allows to describe the change of the radio signal as function of the distance to the shower axis. Furthermore, it has also been shown that the percentile

PoS(ICRC2015)381

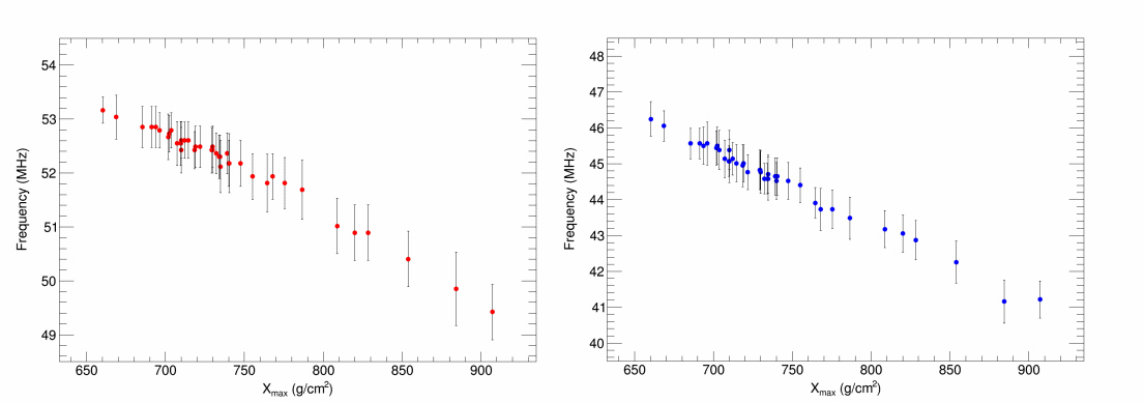

Figure 6: Frequency distribution of the 50th percentile for forty simulated showers. For each shower, the frequency of the 50th percentile has been evaluated as the average of the antennas at 200 m distance (*left*), and 300 m distance (*right*) from the shower axis. The errors correspond to the RMS of the 50th percentile frequency distribution for the antennas at 200 m and 300 m distance respectively.

can be used for studying changes of the frequency spectrum for different values of X_{max} .

The final aim is to find a way, in the energy range $10^{16} - 10^{18}$ eV, to measure cosmic ray energy and mass composition through the analysis of radio signals in the frequency-domain. LOFAR, with its high density of antennas, provides a unique place to perform this measurement. This will be carried out by applying the method described in section 4 to all data detected by LOFAR since 2011. As a cross-check, sets of simulations with protons and iron nuclei as primary particles will be created for each detected shower. All simulated showers will have, as initial parameters, the energy and arrival direction extrapolated from real events detected by LOFAR.

Acknowledgments

The LOFAR cosmic ray key science project acknowledges funding from an Advanced Grant of the European Research Council (FP/2007-2013) / ERC Grant Agreement n. 227610. The project has also received funding from the European Research Council (ERC) under the European Union's Horizon 2020 research and innovation programme (grant agreement No 640130). We furthermore acknowledge financial support from FOM, (FOM-project 12PR304) and NWO (VENI grant 639-041-130). AN is supported by the DFG (research fellowship NE 2031/1-1).

LOFAR, the Low Frequency Array designed and constructed by ASTRON, has facilities in several countries, that are owned by various parties (each with their own funding sources), and that are collectively operated by the International LOFAR Telescope foundation under a joint scientific policy.

PoS(ICRC2015)381

References

[1] J.V. Jelley et al., *Radio pulses from extensive cosmic-ray air showers*, *Nature* **205**: 327 − 328, 1965

[2] D. Ardouin et al., *Radio-detection signature of high-energy cosmic rays by the CODALEMA experiment*, *Nuclear Instruments and Methods in Physics Research*, A **555**: 148 − 163, 2005

[3] H. Falcke et al. *Detection and imaging of atmospheric radio flashes from cosmic ray air showers*, *Nature* **435**: 313 − 316, 2005

[4] M.P. van Haarlem et al., *LOFAR: The Low-Frequency ARray*, *Astronomy & Astrophysics* **556**, A2, 53, 2013 [arXiv:1305.3550]

[5] H.R. Allan, *Radio Emission From Extensive Air Showers*, *Progress in Elementary Particle and Cosmic Ray Physics* **10**: 171 − 302, 1971

[6] H. Falcke and P.W. Gorham, *Detecting Radio Emission from Cosmic Ray Air Showers and Neutrinos with a Digital Radio Telescope*, *Astroparticle Physics* **19**: 477 − 494, 2003

[7] T. Huege and H. Falcke, *Radio-Emission from Cosmic Ray Air Showers: Coherent Geosynchrotron Radiation*, *Astronomy & Astrophysics* **412**: 19 − 34, 2003

[8] T. Huege and H. Falcke, *Radio emission from cosmic ray air showers. Monte Carlo simulations*, *Astronomy & Astrophysics* **430**: 779 − 798, 2005

[9] A. Nigl et al., *Frequency spectra of cosmic ray air shower radio emission measured with LOPES*, *Astronomy & Astrophysics* **488**: 807 − 817, 2008

[10] S. Thoudam et al., *LORA: A scintillator array for LOFAR to measure extensive air shower*, *Nuclear Instruments and Methods in Physics Research* A **767**, 339, 2014

[11] P. Schellart, A. Nelles et al., *Detecting cosmic rays with the LOFAR radio telescope*, *Astronomy & Astrophysics* **560**, A98, 2013 [arXiv:1311.1399]

[12] G.A. Askaryan, *Excess Negative Charge of an Electron-Photon Shower and its Coherent Radio Emission*, *Journal of Experimental and Theoretical Physics*, **14**: 441 − 443, 1962

[13] O. Scholten, K. Werner, and F. Rusydi, *A macroscopic description of coherent geo-magnetic radiation from cosmic-ray air showers*, *Astroparticle Physics* **29**: 94 − 103, 2008

[14] K. Werner and O. Scholten, *Macroscopic Treatment of Radio Emission from Cosmic Ray Air Showers based on Shower Simulations*, *Astroparticle Physics* **29**: 393 − 411, 2008 [arXiv:0712.2517]

[15] D. Heck, *Report FZKA* **6019**, 1998

[16] G. Battistoni et al. in proceedings of *AIP Conference* **896**, 31, 2007

[17] S. Ostapchenko, *QGSJET-II: towards reliable description of very high energy hadronic interactions*, *Nuclear Physics B - Proceedings Supplements* **151**, 147, 2006

[18] T. Huege, M. Ludwig, and C. James, in proceedings of *AIP Conference* **1535**, 128 − 132, 2012

[19] K.D. de Vries, O. Scholten, K. Werner, *The air shower maximum probed by Cherenkov effects from radio emission*, *Astroparticle Physics*, **45**: 23 − 27, 2013 [arXiv:1304.1321]

[20] A. Nelles et al., *A parametrization for the radio emission of air showers as predicted by CoREAS simulations and applied to LOFAR measurements*, *Astroparticle Physics* **60**, 13 − 24, 2014 [arXiv:1402.2872]

PoS(ICRC2015)381